

Semi-inclusive deep-inelastic scattering with CLAS12 at JLab

Gregory Matousek^{a,*}

^a*Duke University,
120 Science Drive, Durham, NC 27708, USA*

E-mail: gregory.matousek@duke.edu

Semi-Inclusive Deep Inelastic Scattering (SIDIS) is a powerful method for studying transverse momentum-dependent parton distribution functions (TMDs) and fragmentation functions (FFs). This paper reviews the ongoing SIDIS program using the CLAS12 spectrometer at Jefferson Lab, which enables precise, multidimensional measurements of cross sections and spin asymmetries in the valence quark regime. By utilizing different unpolarized, longitudinally, and, in the future, transversely polarized targets in combination with a polarized electron beam, CLAS12 provides access to all structure functions relevant to SIDIS. This contribution will focus on both single-hadron and di-hadron SIDIS preliminary and published measurements across a broad range of Q^2 , x_B , z , and P_T . The current status of these studies and their theoretical implications will be discussed in detail.

*31st International Workshop on Deep Inelastic Scattering (DIS2024)
8–12 April 2024
Grenoble, France*

*Speaker

1. Introduction

Electron scattering experiments like those performed at CLAS12 (CEBAF Large Acceptance Spectrometer) are valuable tools for studying the dynamical properties of quarks within a nucleon. These properties are commonly encoded in Transverse Momentum Dependent (TMD) Parton Distribution Functions (PDFs) that map out the three dimensional distribution of partons within the nucleon in terms of their intrinsic transverse momentum k_{\perp} and longitudinal momentum fraction x [1]. Semi-inclusive deep inelastic scattering (SIDIS) at CLAS12 is used to access TMD PDFs by measuring the scattered electron and detecting a hadron (or two in the case of dihadron SIDIS) in the final state. The differential cross section for the described process, drawn in Fig. 1, involves a transverse momentum space convolution of the PDFs and a similar object called fragmentation functions (FFs). At leading twist, FFs describe the probability that a quark with a particular polarization will produce a hadron.

CLAS12 is a fixed target laboratory with near full azimuthal coverage and broad scattering

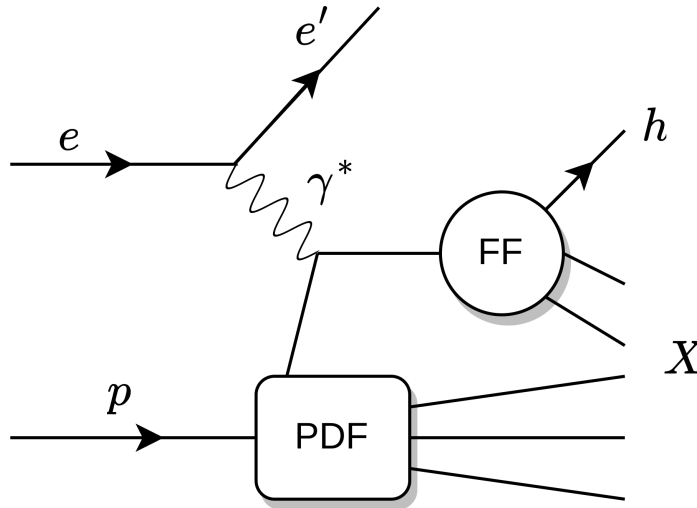


Figure 1: Schematic drawing of the SIDIS process. In single hadron SIDIS, h represents a single final state hadron (ex: π^+). In dihadron SIDIS, two hadrons are measured in the final state.

angle coverage, handled by a forward tagger, a forward detector (most commonly used for measurements discussed here), and a central detector [2]. A toroidal magnetic field bends charged tracks in the forward detector ($5 < \theta < 35^\circ$) which itself is comprised of six identical azimuthal sectors. In each sector, tracks are reconstructed by hits in the drift chamber, and clusters are formed by localized hits in the electromagnetic calorimeters. Particle identification is supplemented by a cherenkov counter, a time-of-flight detector, and in 1-2 sectors (depending on the timeline of the experiment) a RICH detector. In total, CLAS12 is capable of reconstructing and identifying electrons, photons, neutrons, and an array of charged hadrons.

1.1 SIDIS Observables

The differential cross section for single hadron SIDIS is described by the variables Q^2 , x_B , y , z , P_T and the angles ϕ between the electron scattering plane and the hadron production plane, as

well as the angle ϕ_S between the electron scattering plane and the transverse component of the spin vector of the target nucleon. At leading twist, it is written in terms of model-independent structure functions by (see Ref. [3] for the full equation)

$$\begin{aligned}
\frac{d\sigma}{dx dy d\phi_S dz d\phi dP_T} \propto & F_{UU,T} + \epsilon F_{UU,L} \\
& + \sqrt{2\epsilon(1+\epsilon)} \cos\phi F_{UU}^{\cos\phi} + \epsilon \cos 2\phi F_{UU}^{\cos 2\phi} + \lambda_e \sqrt{2\epsilon(1-\epsilon)} \sin\phi F_{LU}^{\sin\phi} \\
& + S_L \left[\sqrt{2\epsilon(1+\epsilon)} \sin\phi F_{UL}^{\sin\phi} + \epsilon \sin 2\phi F_{UL}^{\sin 2\phi} \right] \\
& + S_L \lambda_e \left[\sqrt{1-\epsilon^2} F_{LL} + \sqrt{2\epsilon(1-\epsilon)} \cos\phi F_{LL}^{\cos\phi} \right] \\
& + S_T \left[\sin(\phi - \phi_S) \left(F_{UT,T}^{\sin(\phi-\phi_S)} + \epsilon F_{UT,L}^{\sin(\phi-\phi_S)} \right) + \dots \right] \\
& + S_T \lambda_e \left[\sqrt{1-\epsilon^2} \cos(\phi - \phi_S) F_{LT}^{\cos(\phi-\phi_S)} + \dots \right]. \tag{1}
\end{aligned}$$

where λ_e is the electron beam helicity, S_L is the longitudinal spin of the target (with respect to the virtual photon), S_T is the transverse spin of the target, and ϵ is the ratio of the longitudinal and transverse virtual photon flux. While the structure functions F themselves form our observables, their composition is typically made up of one or more convolutions of PDFs and FFs. Furthermore, their dependence on x , Q^2 , z and P_T is non-trivial, requiring careful multi-dimensional analyses to disentangle their full contributions to the cross section.

CLAS12's high luminosity and wide kinematic coverage offers statistical precision in the multi-dimensional binning of SIDIS structure functions. The broad experimental program is separated into different run groups (RG's) depending on the target configuration, beam energy, and minor detector tweaks. For most run groups, apart from RG-K, the beam energy is typically around 10.6 GeV with 4 – 10nA of beam current. Below in Tab 1. we summarize the run groups and the SIDIS observables they are sensitive to. Run groups A, B, C, and K have collected data, and RG-H is scheduled to take data in 2029 [4].

Run Group	Target	SIDIS Observables
A	un-polarized liq. hydrogen	unpolarized cross sections, F_{LU}
B	un-polarized liq. deuterium	same as RG-A, but u/d flavor separation
C	longitudinally polarized NH ₃ , ND ₃	F_{UL}, F_{LL}
K	un-polarized liq. hydrogen	$F_{UU,L} - F_{UU,T}$ separation (with RG-A)
H	transversely polarized NH ₃	F_{UT}, F_{LT}

Table 1: CLAS12 run groups relevant for SIDIS studies.

2. Single Hadron SIDIS

2.1 Pion Beam Spin Asymmetries

The structure function ratio $F_{LU}^{\sin\phi}/F_{UU}$ was measured by observing beam spin asymmetries in the reaction $ep \rightarrow e'\pi X$. The unpolarized F_{UU} term in leading order is proportional to a convolution of the well studied unpolarized f_1 PDF and the unpolarized fragmentation function D_1 ,

whereas the $F_{LU}^{\sin\phi}$ term is written as a convolution (ζ) of several PDFs (green) and fragmentation functions (blue)[3].

$$F_{LU}^{\sin\phi} = \frac{2M}{Q} \zeta \left(-\frac{\hat{h} \cdot \vec{k}_T}{M_h} \left(x e H_1^\perp + \frac{M_h}{M} f_1 \frac{\tilde{G}^\perp}{z} \right) + \frac{\hat{h} \cdot \vec{p}_T}{M} \left(x g^\perp D_1 + \frac{M_h}{M} h_1^\perp \frac{\tilde{E}}{z} \right) \right). \quad (2)$$

The dominant terms are expected to be those with twist-3 PDFs convoluted with twist-2 FFs. These are eH_1^\perp where H_1^\perp is the Collins FF and the $g^\perp D_1$ where g^\perp is the Sivers-like T-odd PDF. The remaining terms, being convolutions of twist-2 PDFs and twist-3 FFs, are believed to be small in comparison.

Since $F_{LU}^{\sin\phi}/F_{UU}$ is a complex convolution of several PDF and FF pairs, disentangling its relative contributions across a wide, fully differentiable kinematic range is required. The first published results of such a measurement were made for single π^+ SIDIS in Ref. [5]. A preliminary analysis has extended these results to π^0 and π^- , shown in Fig. 2. It can be observed in some kinematic regions that the structure function ratios for π^+ and π^0 are positive and similar in magnitude. This shows that the Collins term eH_1^\perp is not the sole contributor, as the hierarchy $F_{LU}^{\sin\phi}(\pi^-) < F_{LU}^{\sin\phi}(\pi^0) = 0 < F_{LU}^{\sin\phi}(\pi^+)$ would be expected. This behavior is not captured by models, and indicates a significant contribution of additional terms such as $g^\perp D_1$. Ongoing studies have shown an additional contribution may be from exclusive ρ production.

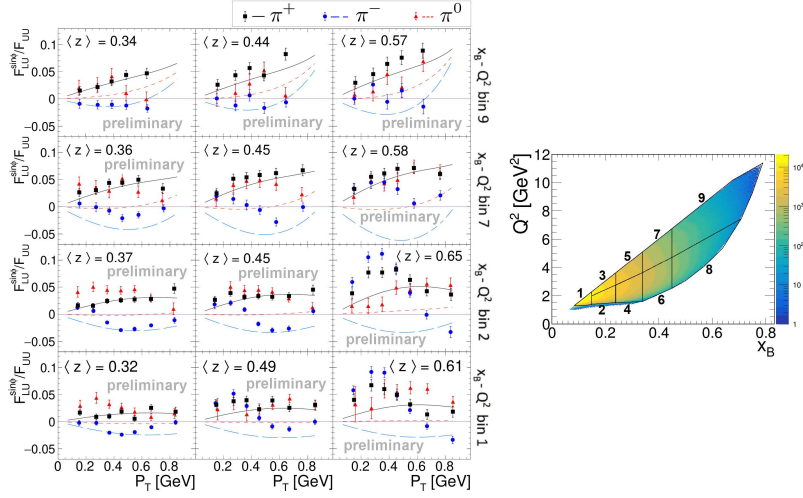


Figure 2: Preliminary results for the structure function ratio $F_{LU}^{\sin\phi}/F_{UU}$ as a function of P_T for selected multidimensional bins of z , Q^2 , and x_B for π^+ (black), π^- (blue), and π^0 (red) [12]. The solid and dashed lines show TMD-based predictions based on the models in Refs. [6, 7] with the color corresponding to the meson.

2.2 Kaon Beam Spin Asymmetries

The analysis of the structure function ratio $F_{LU}^{\sin\phi}/F_{UU}$ has been extended to the strange sector in the form of kaon SIDIS [8]. This study explores the strange-quark TMDs and the differences of the fragmentation into pions and kaons. π - K separation was improved using a neural network that trained on parameters such as detector-level timings, energy depositions and shower profiles in the

calorimeter layers, and reconstructed particle 3-momentum. Figure 3 shows preliminary results for the kaon SIDIS structure function ratio in four dimensional bins. We see that while the $F_{LU}^{\sin\phi}/F_{UU}$ for K^+ and π^+ are both positive, at small z , the K^+ asymmetry is larger. Model comparison gives us insight, as the second model (red) has better agreement with what is seen in data.

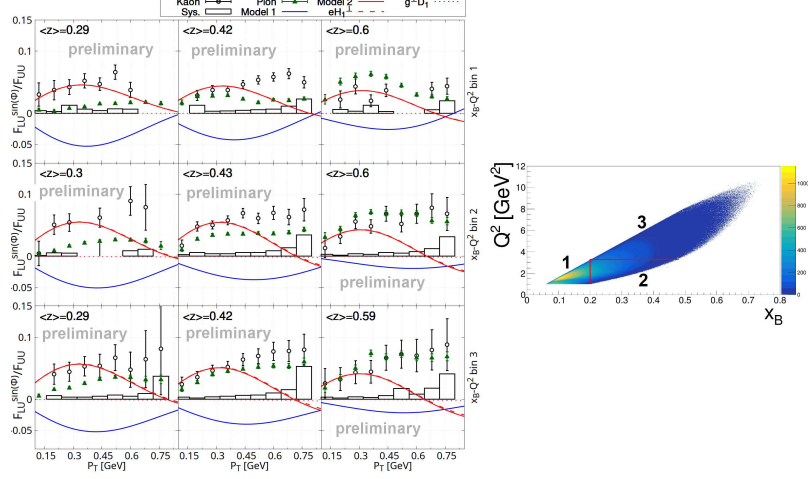


Figure 3: Preliminary results for kaon SIDIS $F_{LU}^{\sin\phi}/F_{UU}$ (open circles) in comparison to π^+ SIDIS (green triangles) as a function of P_T in multidimensional bins of x_B , Q^2 and z [8]. The models are given in Refs. [6, 7].

2.3 ρ Beam Spin Asymmetries

Vector mesons (VMs) influence single hadron SIDIS measurements because of their decay products. The pions originating from the decay of VMs such as ρ^+ and ρ^0 are backgrounds to the single pion SIDIS measurements. Preliminary measurements in the $ep \rightarrow e'\rho^{(+/0)}(n/p)$ exclusive limit have shown that the magnitude of structure function ratios $F_{LU}^{\sin\phi}/F_{UU}$ for ρ^+ and ρ^0 are comparable and at times larger than the pion BSAs (see Fig. 4). Gluon channel ρ^0 production is argued to be mechanism for the sudden asymmetry dip at high z (low four-momentum transfer $|t|$), one that is not present for exclusive ρ^+ due to charge conservation. Studies have shown the strong ρ asymmetries are carried by the decay pions and may contaminate our BSAs. Further work is ongoing, looking into how these asymmetries are folded into the existing pion BSAs and how to subtract them.

2.4 Pion Multiplicities and Unpolarized Modulations

Further studies looking into TMD structure in the proton and in hadronization look at the unpolarized multiplicities and $\cos\phi$ and $\cos 2\phi$ azimuthal modulations of the unpolarized SIDIS cross section. Multiplicities are defined by the ratio of the 4-fold SIDIS different cross section by the 2-fold (x_B , Q^2) differential DIS cross section. Integrated over ϕ , unpolarized single hadron SIDIS measurements are sensitivity to the familiar convolution $F_{UU,T} = \zeta [f_1 D_1]$ [3]. TMD phenomena such as the Boer-Mulders effect and the Cahn effect predict the existence of modulations in the unpolarized cross section. Multidimensional binning of these unpolarized $F_{LU}^{\cos\phi}$ and $F_{LU}^{\cos 2\phi}$ structure functions using Bayesian unfolding in π^+ [9] and π^0 [10] are in progress.

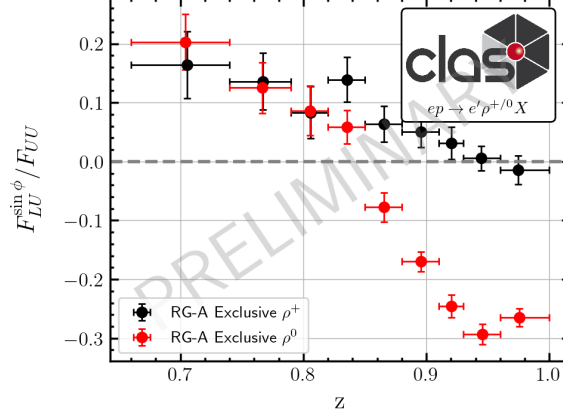


Figure 4: Preliminary results for ρ^+ and ρ^0 SIDIS $F_{LU}^{\sin\phi}/F_{UU}$ in the exclusive limit, binned in the ρ 's z .

3. Dihadron SIDIS

3.1 Dipion Beam Spin Asymmetries

The azimuthal modulations of the dihadron SIDIS cross section are defined using two angles, ϕ_h , related to the total momentum $\vec{P}_h = \vec{P}_1 + \vec{P}_2$ and ϕ_R , related to the relative momentum $\vec{R} = \frac{1}{2}(\vec{P}_1 - \vec{P}_2)$ [11]. The additional degrees of freedom in dihadron SIDIS allow for a more targeted access to twist-3 PDFs as some of their structure functions are less complex compared to those in Eq. 2. In particular, the $A_{LU}^{\sin\phi_R}$ BSA is sensitive to eH_1^\perp without a convolution over transverse momentum space. Additionally, dihadron SIDIS convolutes the TMD PDFs with new objects called dihadron FFs (DiFFs). Some DiFFs, such as the fragmenting quark helicity-dependent G_1^\perp , have no single hadron SIDIS counterpart at leading twist and can be accessed through $A_{LU}^{\sin(\phi_h - \phi_R)}$, among other amplitudes.

In a CLAS published $ep \rightarrow e'\pi^+\pi^-X$ dihadron study, several amplitudes including $A_{LU}^{\sin\phi_R}$ and $A_{LU}^{\sin(\phi_h - \phi_R)}$ were extracted as a function of x , z , and M_h [12]. From this data, a point-by-point extraction of the twist-3 PDF, $e(x)$, was performed [13]. In combination with measurements on a deuteron target, flavor decomposition (u/d) of $e(x)$ will be performed. The dihadron program at CLAS has recently expanded to cover $e\pi^\pm\pi^0$ (which is under internal review), $eK\pi$ and eKK final states to explore quark flavor and hadron type dependence in the DiFFs. Ongoing studies of dihadron production with a longitudinally polarized target will also perform the first extraction of a twist-3 DiFF, \tilde{G} , which encodes quark-gluon correlations in hadronization.

3.2 Back to Back Dihadrons

The traditional SIDIS picture describes the struck quark forming the final state hadrons using Fragmentation Functions. On the other hand, Fracture Functions describe (at leading twist) the probability the target remnant will form a hadron h given a struck quark flavor q_f [14]. The conditional probability implies there is no soft/hard scale separation, thus factorization does not hold. The PDFs in single hadron SIDIS can be obtained by performing an integral over the fractional

longitudinal nucleon momentum ζ . For example,

$$\sum_h \int_0^{1-x} d\zeta \zeta \hat{l}_{1L}(x, \zeta) = (1-x)g_{1L}(x) \quad (3)$$

where $\hat{l}_{1L}(x, \zeta)$ is the fracture function and $g_{1L}(x)$ is the helicity distribution. Understanding target fragmentation is crucial for forming the complete picture of hadronization.

Beam spin asymmetries of back-to-back π^+p pairs have been published at CLAS12 [15]. Correlations between the target breakup proton and the π^+ formed during the struck quark's hadronization were observed through modulations of $\Delta\phi$, the azimuthal angle difference between the p and π^+ in the $\gamma-N$ center-of-mass frame. The structure functions for this process are sensitive to convolutions of leading twist fracture functions \hat{u}_1 and $\hat{l}_1^{\perp h}$ (of the proton) and the unpolarized fragmentation function D_1 (of the pion). These measurements are a first look in dihadron production to a previously unobserved leading-twist spin and TMD fracture function and provide a new avenue for studying nucleonic structure and hadronization.

3.3 Lambda Polarization

The Λ longitudinal spin transfer coefficient D_{LL}^Λ , which encodes the probability for a struck quark to impart its polarization to the produced Λ , has been studied in the valence region at CLAS12. Being the most precise to date measurement, the study finds a small positive, yet consistent with zero result [16]. The results are also consistent with the Constituent Quark Model of the Λ which argues the spin of the Λ is carried entirely by its strange quark. A graph neural network (GNN) was developed in the CLAS study to address the large background spectrum underneath the Λ signal distribution due to combinatoric $p\pi^-$ pairs [17].

4. Conclusion

In conclusion, the CLAS12 detector at Jefferson Lab offers unprecedented capabilities for studying the internal structure of nucleons through SIDIS measurements. With its high luminosity and wide kinematic coverage, CLAS12 enables detailed, multidimensional analyses of transverse momentum-dependent parton distribution functions (TMD PDFs) and fragmentation functions (FFs). With several studies utilizing the recently collected longitudinally polarized data underway, the ongoing and future analyses with CLAS12 will continue to significantly advance our understanding of parton dynamics and hadronization mechanisms in the valence region.

References

- [1] Boussarie, Renaud and Burkardt, Matthias and Constantinou, Martha and others. TMD Handbook. URL <http://arxiv.org/abs/2304.03302>.
- [2] Burkert, V.D. and Elouadrhiri, L. and Adhikari, K.P. and others. The CLAS12 Spectrometer at Jefferson Laboratory. 959:163419. ISSN 01689002. doi: 10.1016/j.nima.2020.163419. URL <https://linkinghub.elsevier.com/retrieve/pii/S0168900220300243>.

- [3] Bacchetta, Alessandro and Diehl, Markus and Goeke, Klaus and others. Semi-Inclusive Deep Inelastic Scattering at Small Transverse Momentum. 2007(02):093–093. ISSN 1029-8479. doi: 10.1088/1126-6708/2007/02/093. URL <http://arxiv.org/abs/hep-ph/0611265>.
- [4] D. Higinbotham. Jefferson Lab’s 12GeV Experimental Schedule, talk at the CLAS CM March 2024. <https://indico.jlab.org/event/829/contributions/14068/attachments/10719/16238/Higinbotham%20-%20Experimental%20Schedule%20and%20Future%20Directions.pptx>, 2024. Accessed: 2024-10-08.
- [5] S. Diehl and A. Kim and G. Angelini et al. Multidimensional, High Precision Measurements of Beam Single Spin Asymmetries in Semi-inclusive π^+ Electroproduction off Protons in the Valence Region. *Physical Review Letters*, 128(6):062005, feb 2022. ISSN 0031-9007, 1079-7114. doi: 10.1103/PhysRevLett.128.062005.
- [6] W. Mao and Z. Lu. Twist-3 quark-gluon-quark correlation functions and single spin asymmetries in semi-inclusive DIS. *Eur. Phys. J. C*, 73:2557, 2013. doi: 10.1140/epjcs/10052-013-2557-9.
- [7] W. Mao and Z. Lu. Theoretical study of twist-3 effects in polarized SIDIS. *Eur. Phys. J. C*, 74:2910, 2014. doi: 10.1140/epjcs/10052-014-2910-7.
- [8] A. Kripko and S. Diehl and CLAS Collaboration. To be published, presented at the Workshop on Present and Future Perspectives in Hadron Physics, Frascati, 2024. Available at: https://agenda.infn.it/event/38467/contributions/234436/attachments/122303/178823/Kaon_Kripko_workshop2024.pdf.
- [9] R. Capobianco. Measurements of the $\text{Cos}\phi_h$ and $\text{Cos}2\phi_h$ Moments of the Unpolarized SIDIS π^+ Cross-section at CLAS12. In *Proceedings of the International Workshop on CLAS12 Physics and Future Perspectives at JLab*, Paris, France, 2023. URL <https://indico.ijclab.in2p3.fr/event/9131/contributions/28970/>. Also presented at the 2023 Fall Meeting of APS DNP and JPS (2023).
- [10] Scott, Marshall and CLAS12 collaboration. Current status of the neutral pion multiplicity studies at CLAS12. In *Proceedings of 25th International Symposium on Spin Physics — PoS(SPIN2023)*, page 068, Durham, NC, USA, July 2024. Sissa Medialab. doi: 10.22323/1.456.0068. URL <https://pos.sissa.it/456/068>.
- [11] Gliske, Stephen and Bacchetta, Alessandro and Radici, Marco. Production of two hadrons in semi-inclusive Deep Inelastic Scattering. *Physical Review D*, 90(11):114027, December 2014. ISSN 1550-7998, 1550-2368. doi: 10.1103/PhysRevD.90.114027. arXiv:1408.5721 [hep-ex, physics:hep-ph, physics:nucl-ex, physics:nucl-th].
- [12] Hayward, T.B. and Dilks, C. and Vossen, A. and others. Observation of Beam Spin Asymmetries in the Process $ep \rightarrow e'\pi^+\pi^-X$ with CLAS12. *Physical Review Letters*, 126(15):152501, April 2021. ISSN 0031-9007, 1079-7114. doi: 10.1103/PhysRevLett.126.152501.

- [13] Courtoy, Aurore and Miramontes, Angel and Avakian, Harut and others. Extraction of the higher-twist parton distribution $e(x)$ from CLAS data. (arXiv:2203.14975), March 2022. URL <http://arxiv.org/abs/2203.14975>. arXiv:2203.14975.
- [14] Chen, K.B. and Ma, J.P. and Tong, X.B. Twist-3 contributions in semi-inclusive DIS in the target fragmentation region. *Physical Review D*, 108(9):094015, November 2023. ISSN 2470-0010, 2470-0029. doi: 10.1103/PhysRevD.108.094015.
- [15] Avakian, H. and Hayward, T. B. and Kotzinian, A. and others. First observation of correlations between spin and transverse momenta in back-to-back dihadron production at CLAS12. (arXiv:2208.05086), August 2022. URL <http://arxiv.org/abs/2208.05086>. arXiv:2208.05086.
- [16] Matthew McEneaney. Longitudinal spin transfer to Λ hyperons in CLAS12. In *Proceedings of the 24th International Spin Symposium (SPIN2021)*, December 2022.
- [17] M. McEneaney and A. Vossen. Domain-adversarial graph neural networks for Λ hyperon identification with CLAS12. *Journal of Instrumentation*, 18(06):P06002, June 2023.